

MAGNET DIVISION NOTES

Author: R.C. Fernow
Date: February 6, 1984
No.: 40-1
Title: End Fields for the Modified SSC-43D Dipole
Task Force: Coil Geometry Analysis

M. Anerella
F. Atkinson
G. Bagley
A. Bertsche
E. Bläser
D. Brown
V. Buchanan
J. Cottingham
J. Cullen
P. Dahl
Y. Elisman
A. Feltman
R. Fernow
G. Ganetis
D. Gardner
A. Ghosh
C. Goodzeit
D. Gough
A. Greene
H. Hahn
W. Harrison
J. Herrera

R. Hogue
S. Kahn
E. Kelly
H. Kirk
J. Koehler
R. Louttit
R. LeRoy
W. McGahern
G. Morgan
R. Palmer
S. Plate
I. Polk
A. Prodehl
K. Robins
R. Rosenka
W. Sampson
W. Schneider
M. Shapiro
R. Shutt
J. Skaritka
A. Stevens
C. Sylvester

P. Thompson
P. Wanderer
T. Wild
E. Willen

A new study of the end fields of the prototype SSC-43 dipole became necessary because of three developments: 1) the use of two currents instead of the original three, 2) a change in the relative spacing of the inner and outer saddle regions, and 3) a mistake in the early version of the computer program MAG3, which effectively reduced the contribution of current elements in the dogbone region of the end.¹ We refer to the coil configuration resulting from items 1) and 2) above as design SSC-43D. The 2D cross section is identical to SSC-43.²

The SSC-43D straight section conductor blocks and currents are listed in Table I. The inner coil is run at 5.17 kA and the outer coil is run at 7.18 kA, producing a central field of 76.7 kG with saturated iron. The straight section margins above critical current are listed in Table I. The critical block is the one in the inner coil nearest the post. A negative consequence of dropping the third independent current is that the outer coil midplane block will now have much more current margin than the other blocks. A second unpleasant consequence is that the field produced by the new current distribution produces a very large negative b_2 , as shown in Table II.

We have used the program MAG3 to examine the peak fields, fringe fields, multipole content, cross talk, and longitudinal forces for the ends of the SSC-43D dipole. It should be kept in mind that this program calculates fields for conductors only (no iron). Figure 1 shows the fields in the region of the conductors in the 2D part of the magnet for the midplane (\square), post angle of the outer coil ($^\circ$), and post angle of the inner coil (Δ). The open symbols are from calculations using MDP, the standard 2D, saturable iron program at BNL. It can be seen that the field reversal point occurs near $r = 2.9$ cm. The closed symbols are from the program MAG3. The two calculations for B_y differ by a roughly constant off-set. We present this comparison here to show that the MAG3 calculations are reasonable, and to show how the presence of iron might alter the results. We don't yet have a program to make detailed checks of the MAG3 calculations in the magnet ends.

The dimensions of the dogbone transition piece is shown in Figure 2. We have approximated this shape with a single cone since field calculations performed with both shapes agreed to better than 1%. Figure 3 shows a plot of arc length versus longitudinal distance for the inner and outer coil end conductors on the large cylinder. The inner coil has a 2-1/4 inches straight section to separate the two layers and lower the inner coil peak field. The x marks the location of the peak field points in the curved parts of the saddles.

An analysis of the effect of the end peak fields on the magnet performance is presented in Table III. The quantity df is the estimated critical current degradation due to bending of the Nb_3Sn cable thru the saddle. It appears that this end design should give a comfortable margin and that the magnet's performance will be limited by the critical current in the straight section.

The maximum and minimum values of H at the conductor centers is shown in Figure 4 as a function of the longitudinal length Z . It is assumed that the straight section ends at $Z=0$. The maximum H climbs slowly to a peak in the saddle region. The peak field point for the curved part of inner coil is ~ 46 kG, approximately at $r = 4.9$ cm, $\phi = 27.2^\circ$, $Z = 36.2$ cm. The peak curved outer coil point is ~ 59 kG, approximately at $r = 5.9$ cm, $\phi = 26.6^\circ$, $Z = 32.9$ cm. Approximately 6 kG of these peak fields is due to the presence of the second magnet in the 2-in-1 configuration. The minimum field regions are of interest for quench protection studies. The field near the midplane in the outer coil is very small.

The fringe field on the midplane is shown in Figure 5. The field in the region of the saddle ($Z = 35$ cm) exceeds 300 G for a distance of 30 cm from the axis.

We have checked the accuracy of the multipole calculations by comparing calculations for the CBA dipoles with measurements.³ The results for B_2 , B_4 and B_6 shown in Figure 6 show that the program reproduces the measured structure versus Z qualitatively, but not quantitatively. Thus the numerical values may be in error by up to a factor of 2.

Table IV and Figure 7 shows the multipoles when the other coil is present in the end. The forbidden harmonics H_1, H_3, \dots are present. The tabulated values of the harmonics are integrated from $Z = 2.5$ to $Z = 52.5$ cm. One should expect the iron to significantly alter the $n = 0$ results at least. The ends give large quadrupole (H_1) and sextupole (H_2) contributions. The H_1 field is entirely due to cross talk from the other 2-in-1 magnet and could be significantly altered by the iron configuration chosen for the end region. The H_2 field is inherently due to the coil configuration, which keeps the turns as close as possible to the midplane thru most of the end region. We make a rough estimate of the importance of these effects by comparing the integrated multipoles for both ends to the dipole $\int B dx$

$$h_n \equiv \frac{2}{B_0 L} (1 \text{ cm})^n \int_{\text{end}} H_n dz$$

where we take $B_0 = 80$ kG and $L = 14.6$ m. This is shown in Table IV. The H_2 field is most important, contributing $\sim 8 \times 10^{-4}$.

A possible remedy to this situation suggested by R. Palmer, is to make the end windings of the outer coil have the same minimum bend radius as the inner coil. One could then make the outer turns follow as closely as possible to the outer post, where they would give a negative H_2 contribution to the end multipoles. We intend to study this suggestion later and the design change could possibly be implemented in a later prototype.

Lastly, we shown in Table V the total force on the conductors for one quadrant of one end of one coil in the 2-in-1. Note that with this end configuration block 1 has an inward directed longitudinal force.

Footnotes and References

1. As a consequence the results presented in Field Computation Notes 32 and 35 should be ignored.
2. R. Fernow, SSC Technical Note No. 4 (1983).
3. H. Kirk, et al., BNL Report 32728 (1983).

TABLE I
Conductor Blocks in Straight Section

Block	N	ϕ_{st}	ϕ_{end}	r (cm)	I (kA)	Current Margin (%)
1	15	0.15°	60.14	2.002	5.17	9
2	3	64.20	76.20	2.002	5.17	3
3	12	0.10	33.92	2.840	7.18	52
4	5	40.37	54.46	2.840	7.18	9

TABLE II
2D Multipoles, $b_n \times 10^4 @ 1 \text{ cm}$

b_2	-77.3
b_4	-1.9
b_6	0.5
b_8	0.0
b_{10}	0.1
B_0 (kG)	76.7 (saturated iron)

TABLE III
End Peak Field Performance

Block	straight		end				
	B_p (kG)	I_{CR} (kA)	B_p (kG)	I_{CR} (kA)	r_{min} (in)	df	$I_{CR} \cdot df$ (kA)
2	82.4	5.33	46	11.8	2.2	1	11.8
			27	14.5	1.4	0.85	12.3
4	66.7	7.84	59	9.3	>1.7	1	9.3

TABLE IV
End Multipoles

N	$\int HndZ$ (kG/cm ⁿ ·cm)	h_n ($\times 10^{-4}$)
0	1525	---
1	16.64	2.8
2	37.90	6.5
3	0.1691	0.0
4	-0.8485	-0.2
5	0.0013	0.0
6	0.0373	0.0

TABLE V
Total Force Per Coil Quadrant Per End (Newtons)

Block	F_ϕ	F_r	F_z
1	-63700	87590	-6065
2	-28870	9330	1165
3	-47610	-19585	11955
4	-53120	-8920	10950

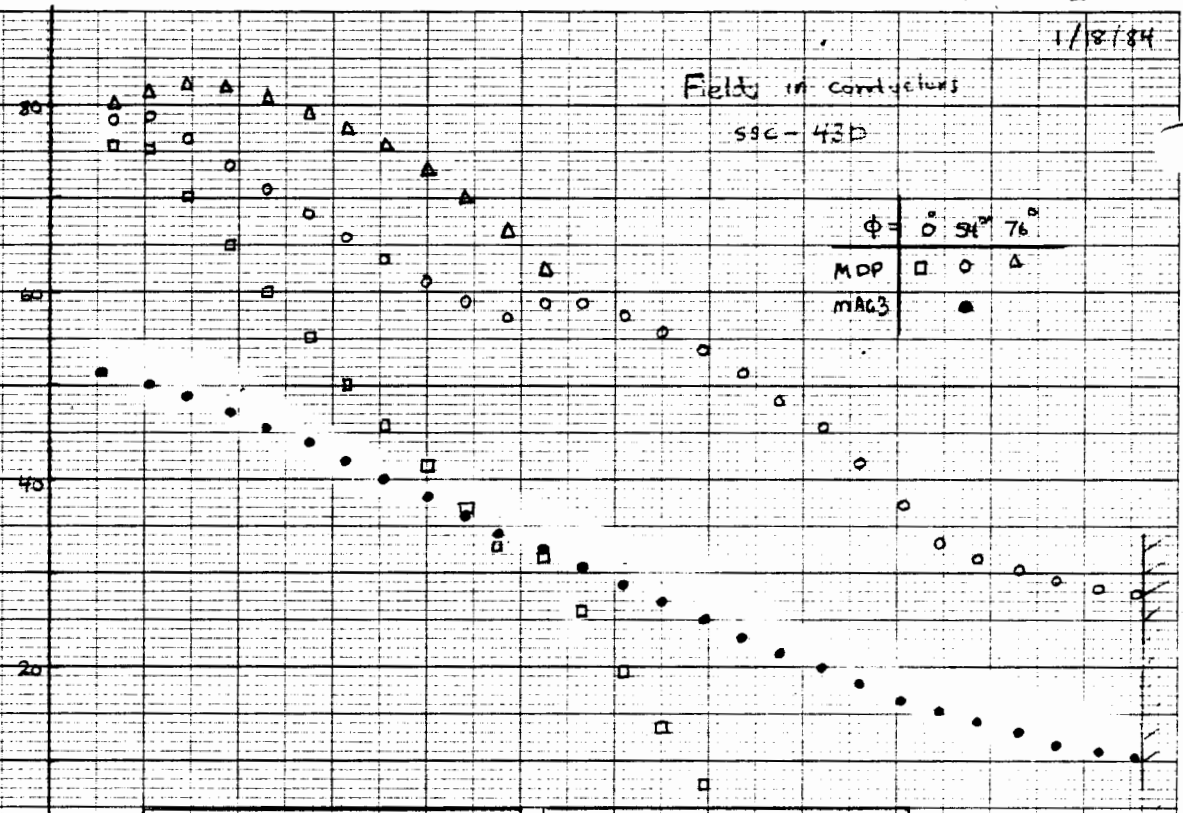
1/18/84

Field in conductors

59C-43D

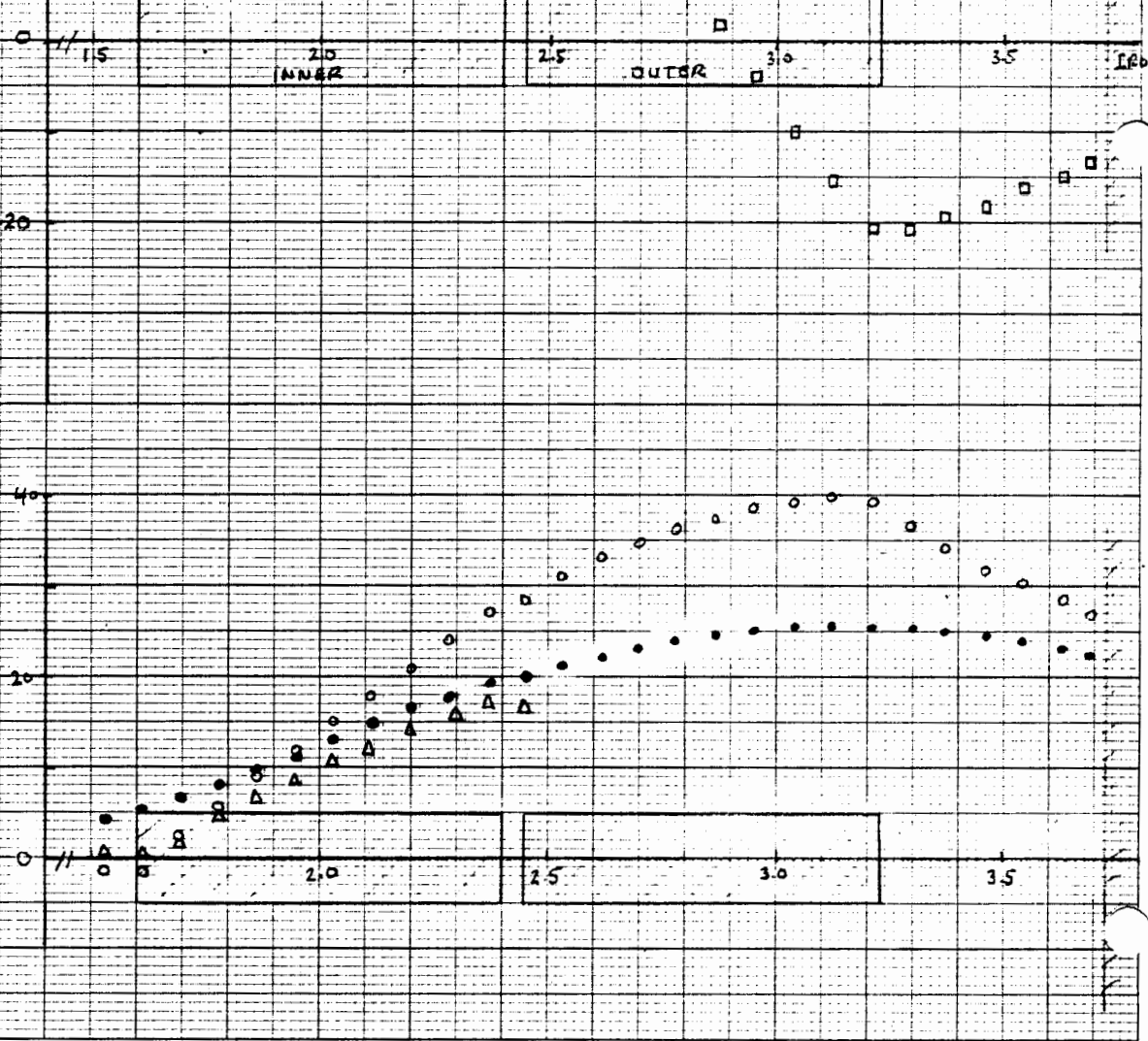
$\phi =$	0°	90°	76°
MDP	\square	\circ	Δ
MAG3		\bullet	

B_y
(KG)



1.5	2.0 INNER	2.5	3.0 OUTER	3.5	IRON
-----	--------------	-----	--------------	-----	------

B_x
(KG)



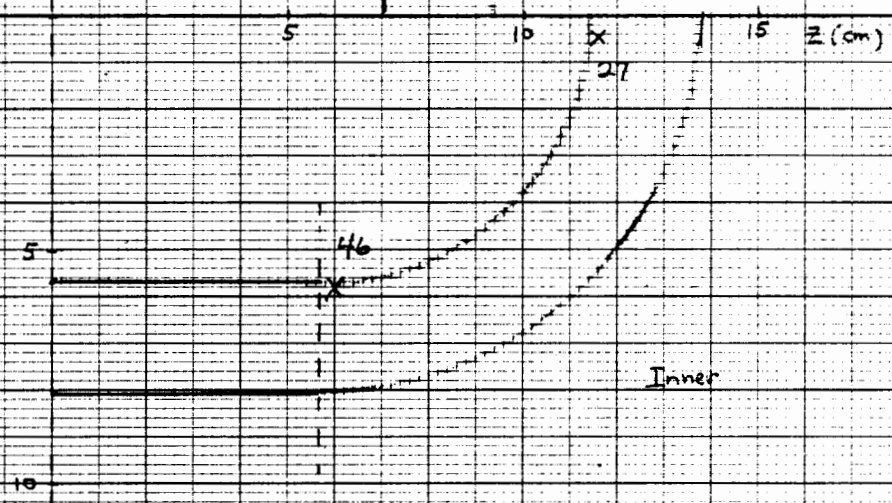
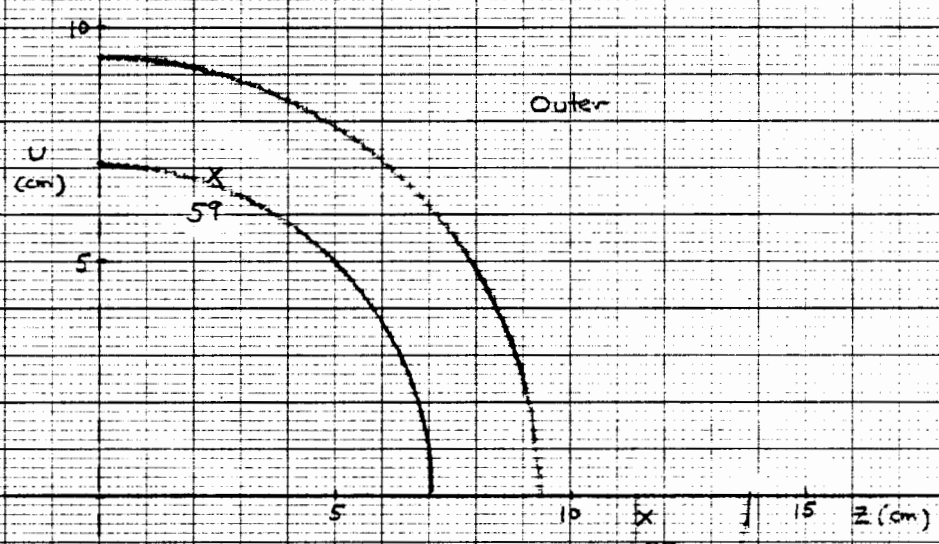
2.0	2.5	3.0	3.5
-----	-----	-----	-----

46 1320

K&E 10 X 10 TO 1/2 INCH 7 X 10 INCHES
KEUFFEL & ESSER CO. MADE IN U.S.A.

1/10/84

SSC-43D



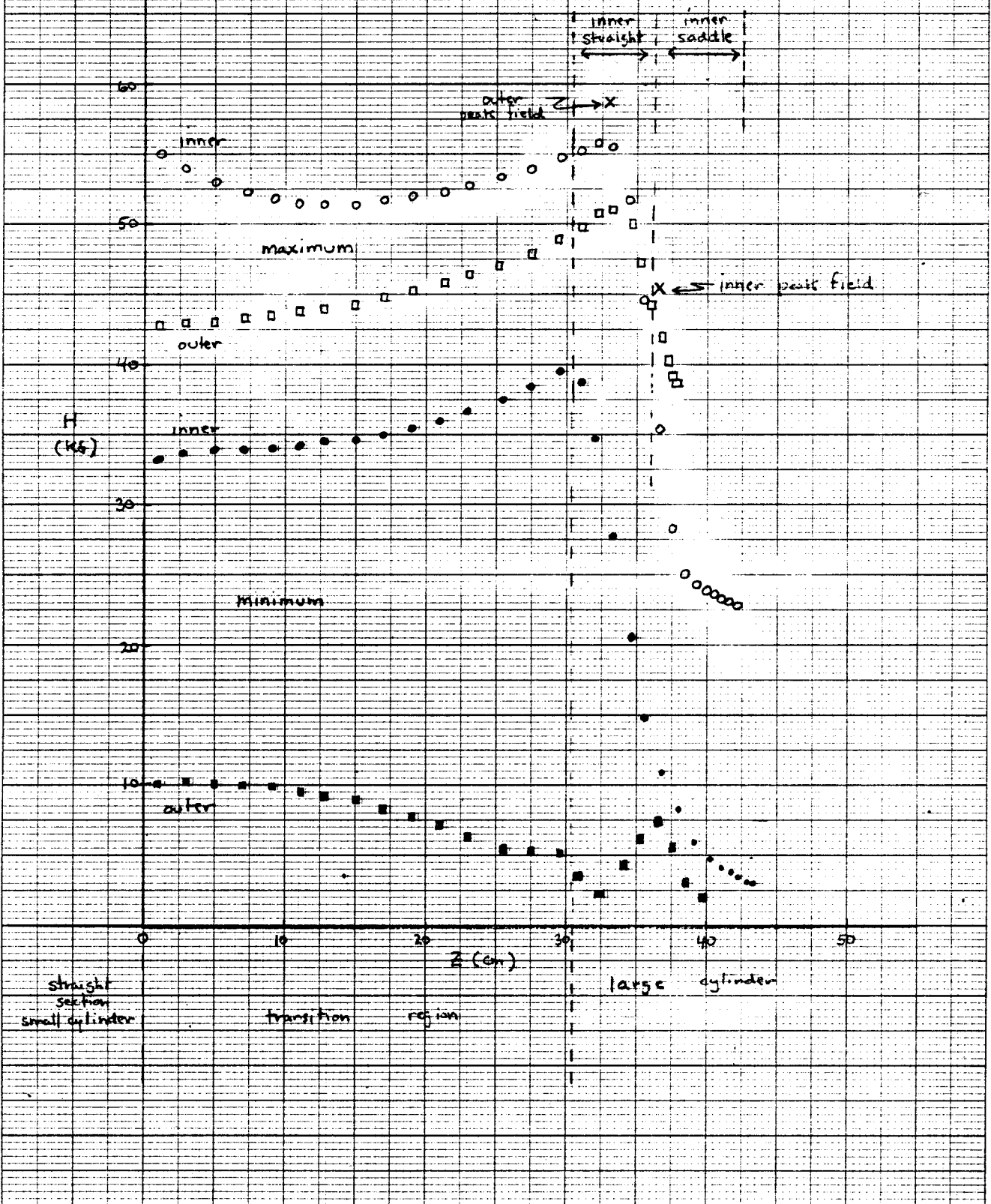
← transition region → ← large cylinder →

46 1320

K&E 10 X 10 TO 1/2 INCH 7 X 10 INCHES KEUFEL & ESSER CO. MADE IN U.S.A.

1/10/84

Fields at conductor element centers
SSC-43D



46 1320

K&E 10 X 10 TO 1/4 INCH 7 X 10 INCHES KEUFFEL & ESSER CO. MADE IN USA

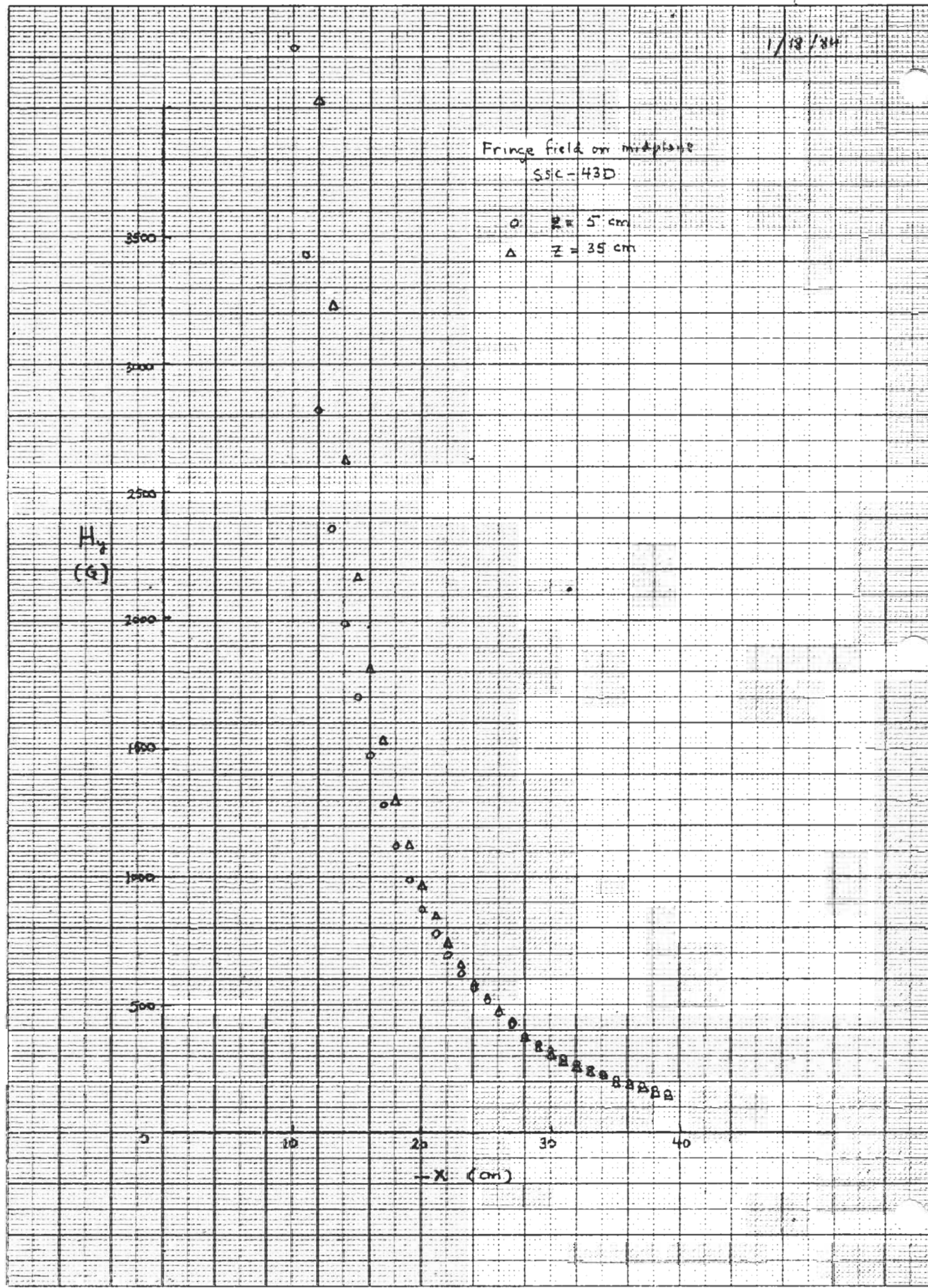
Fringe field on midplane
SSIC-43D

○ $z = 5$ cm
△ $z = 35$ cm

H_z
(G)

3500
3000
2500
2000
1500
1000
500
0

-X (cm)



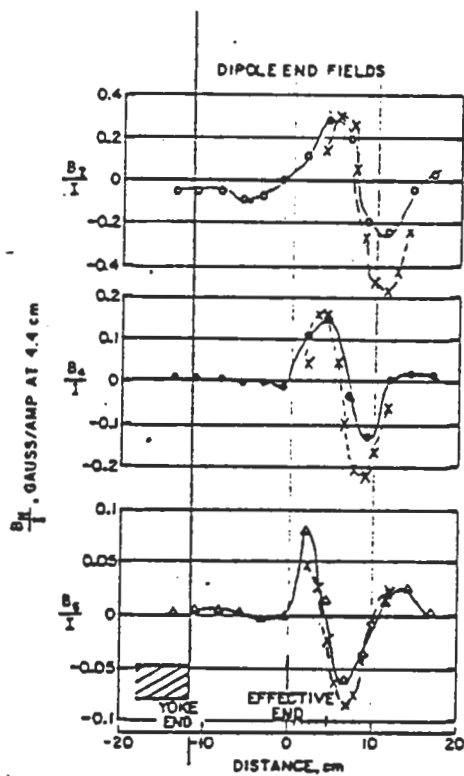
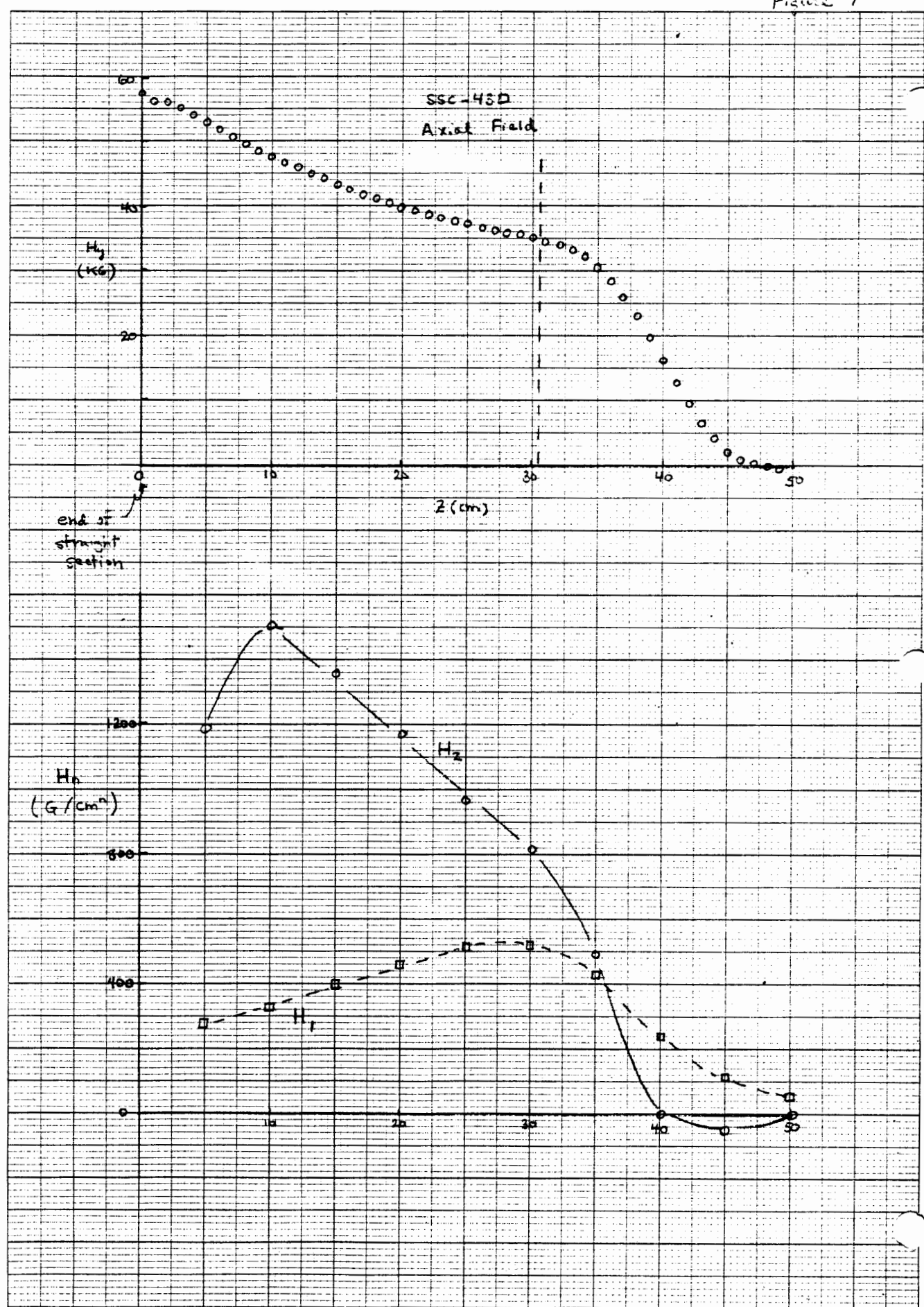


Figure 6. The end field structure of the first three higher allowed harmonics of a dipole magnet.

46 1320

KEE 10 X 10 TO 1/4 INCH 7 X 10 INCHES
KEUFFEL & ESSER CO. MADE IN U.S.A.



end of
straight
section

SSC-45D
Axial Field

H_y
(Kc)

Z (cm)

H_x
(G/cm^2)

H_2

H_1